

Multivariable MPC algorithm with separated prediction horizons : application to simultaneous control of tension and drawing speed in optical fiber manufacturing processes

Olivier Gehan^{*†}, Johannes Reuter[‡], Eric Pigeon^{*}
Mathieu Pouliquen^{*}, Tomas Menard[§], Boubekour Targui^{*}

Abstract

This paper focuses on the multivariable control of a drawing tower process. The nature of the process together with the differences in measurement noise levels that affect the variables to be controlled motivated the development of a new MPC algorithm. An extension of a multivariable predictive control algorithm with separated prediction horizons is proposed. The obtained experimental results show the usefulness of the proposed algorithm..

Key words : model predictive control, multivariable process, separate prediction horizons, drawing process

1 Introduction

Optical fibers are critical components in a multitude of technical applications reaching from communication infrastructure systems to high power laser cutting. In order to minimize losses and optimize optical and mechanical features, several parameters have to be tightly controlled during the manufacturing process. The drawing speed and tension have been identified to be most critical to achieve the desired properties of the optical fiber ([15], [6]). From the control point of view, the system can be regarded as MIMO system exhibiting various delays. Previous work has focused on the SISO control of the fiber diameter [9]. Moreover, in [2] a PID controller is used for set point regulation of the diameter. In this paper, the MIMO case

is taken into account, where the key parameters tension and speed are considered as controlled quantities. While the latter can be controlled directly, the tension is influenced indirectly by the furnace heat power and the preform downfeed speed, leading to a significantly coupled MIMO system, which requires an appropriate multivariable control scheme.

Model Predictive Control (*MPC*) has been widely studied in the literature and the reader can find complete state of the art in ([14], [4]). Extensions of the original works to the nonlinear case led to *NMPC* ([10]). The underlying idea of MPC is quite intuitive as it consists in finding a sequence of future control values that minimizes a quadratic cost function which mainly depends on the tracking errors. Its popularity probably comes from its ability to deal with input or state constraints that reflect physical limitations ([11]). But the solution of the underlying control problem usually needs to be computed on-line and this particularity obliges to fix finite values of prediction horizons to make the problem computationally feasible. This is probably one of the main differences subject to standard H_2 and H_∞ design methods. In the linear case, GPC ([7]) is probably the most famous release of MPC for both SISO and MIMO systems. In the MIMO case, it may be useful to specify the closed loop dynamics independently for the variables to be controlled. This can be the case for example when they defer significantly in regard of their open loop dynamics or when one needs to distinguish the closed -loop bandwidths in the presence of different measurement noise levels. Considering the fact that the parameter which plays one of the most important roles in the definition of the closed - loop dynamics is the prediction horizon, the main theoretical contribution of this paper is to propose a new multivariable linear predictive control law with separated prediction horizons for each output. The results obtained on the process to be controlled,

^{*}LAC EA7478, ENSICAEN, 6 Bd du Marechal Juin, 14050 Caen Cedex, France, olivier.gehan@ensicaen.fr

[†]This work received financial support from the European Union for the LORA project

[‡]HTWG Konstanz, Institute of System Dynamics, Konstanz, Germany, jreuter@htwg-konstanz.de

[§]Mechatronics Department, Rajamangala University of Technology, Thanyaburi, Thailand, tomas.m@rmutt.ac.th

namely the draw tower process, show the usefulness of the proposed approach.

This paper is organized as follows. In the first section, the draw tower process and the control objectives are presented and an identified multivariable control-oriented model is given. The second section is devoted to the multivariable predictive control algorithm with separate prediction horizons and the expression of the linear time-invariant controller is derived. Finally, the experimental results are presented and discussed in section 3. The paper concludes with a summary and few remarks subject to future work.

2 Fiber drawing tower description

The principle of a fiber drawing process is depicted in figure 1. A silica glass cylinder, called the preform, is suspended in a furnace where the temperature and the preform downfeed speed mechanism are controlled. Under the high temperature effects, the preform becomes fluid, a small drop of glass appears on its bottom and the latest one starts to fall due to the gravity effects. This drop is grabbed by the drawing tractors and the process starts. Several treatments are then applied to generate the coated fiber at the bottom of the tower. For that process it is well known that several parameters have significant impact on the optical and mechanical properties of the fiber. Previous work has already been dedicated to the control of the fiber diameter ([9]). But the quality of the fiber is also related to the drawing speed and the fiber tension. A physical study has shown that these parameters can be controlled by means of the preform downfeed speed and the furnace heat power. For this multivariable control problem, the following notations will be used for the rest of the paper

$$\begin{aligned} \bar{y}(t) &= \begin{pmatrix} y_1(t) \\ y_2(t) \end{pmatrix} = \begin{pmatrix} \text{draw speed} \\ \text{fiber tension} \end{pmatrix} \\ \bar{u}(t) &= \begin{pmatrix} u_1(t) \\ u_2(t) \end{pmatrix} = \begin{pmatrix} \text{preform downfeed speed} \\ \text{furnace heat power} \end{pmatrix} \end{aligned} \quad (1)$$

A control-oriented model has been identified on the manufacturing process using a subspace method based on an oblique projection algorithm ([13]). This led to a 4th order discrete-time state-space model with a sampling period $T_e = 80s$. Finally, the available output signals are corrupted by measurement noise, whose normalized variances are $\sigma_1^2 = 0.001$ and $\sigma_2^2 = 0.05$ for the drawing speed and the fiber tension respectively. This difference of range motivates the development of a multivariable control algorithm that enables independent specification of the controlled variables dynamics.

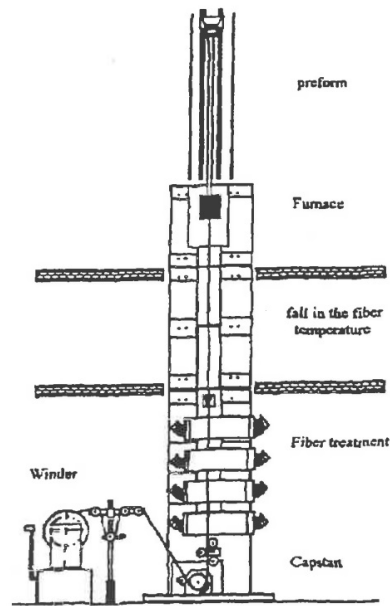


Figure 1: Draw tower process

3 Multivariable Model Predictive Control Algorithm

3.1 Class of systems

Let us consider the class of systems that can be modelled by the following discrete-time ARARMAX [8] multivariable structure

$$\begin{cases} [A(q^{-1})]\bar{y}(t) = [B(q^{-1})]\bar{u}(t-d-1) + \bar{v}(t) \\ [D(q^{-1})]\bar{v}(t) = [C(q^{-1})]\bar{\gamma}(t) \end{cases} \quad (2)$$

where $\bar{y}(t) = [y_1(t) \dots y_p(t)]^T \in \mathbf{R}^p$, $\bar{u}(t-d-1) = [u_1(t-d-1) \dots u_m(t-d-1)]^T \in \mathbf{R}^m$ and $\bar{v}(t) \in \mathbf{R}^p$ respectively denote the vectors of p plant outputs, m control variables, p external disturbances and $\bar{\gamma}(t) = [\gamma_1(t) \dots \gamma_p(t)]^T \in \mathbf{R}^p$ is a vector of sequences of independent random variables with zero mean and finite variances. Finally, q^{-1} denotes the backward shift operator and d is the plant delay in sampling periods. In the following, one shall consider the particular case $m = p$ and decoupled step-like disturbances i.e $D(q^{-1}) = (1 - q^{-1})I_p$ where I_p stands for the Identity matrix. Hence (2) leads to

$$\begin{aligned} [D(q^{-1})][A(q^{-1})]\bar{y}(t) &= [B(q^{-1})]\bar{u}_d(t-d-1) \\ &+ [C(q^{-1})]\bar{\gamma}(t) \end{aligned} \quad (3)$$

with $\bar{u}_d(t) = [D(q^{-1})]\bar{u}(t) = (1 - q^{-1})I_p\bar{u}(t)$. The innovation state-space model [1] associated to (3) is given by

$$\begin{cases} X(t+1) = FX(t) + G\bar{u}_d(t) + E\bar{\gamma}(t) \\ \bar{y}(t) = HX(t) + \bar{\gamma}(t) \end{cases} \quad (4)$$

where $X(t) \in \mathbf{R}^n$ denotes the state vector and $F \in \mathbf{R}^{n \times n}$, $G \in \mathbf{R}^{n \times m}$, $H \in \mathbf{R}^{p \times n}$ and $E \in \mathbf{R}^{n \times p}$

3.2 Control objective with separated prediction horizons

In the literature, the control objective of the standard MPC algorithms usually consists of minimizing, in a receding horizon sense, the following quadratic cost function

$$J_1 = \mathcal{E} \left(\sum_{k=h_i}^{h_p} \bar{y}^T(t+k) Q \bar{y}(t+k) \right) + \mathcal{E} \left(\sum_{k=h_i}^{h_p} \bar{u}_d^T(t+k-h_i) R \bar{u}_d(t+k-h_i) \right) \quad (5)$$

where $\mathcal{E}()$ denotes the mathematical expectation, $h_i \geq d+1$ and h_p are respectively the initialization and prediction horizons and $Q \in \mathbf{R}^{p \times p}$ and $R \in \mathbf{R}^{m \times m}$ can be specified as diagonal matrices such like

$$Q = \text{diag}(q_i), \quad q_i \geq 0; \quad R = \text{diag}(r_i), \quad r_i > 0 \quad (6)$$

To specify independently the closed-loop dynamics of the different outputs, the previous criteria is therefore modified to distinguish the prediction horizons of each output, yielding

$$J_2 = \mathcal{E} \left(\sum_{j=1}^p \sum_{k=h_i}^{h_p(j)} y_j^T(t+k) q_j y_j(t+k) \right) + \mathcal{E} \left(\sum_{k=h_i}^{h_p} \bar{u}_d^T(t+k-h_i) R \bar{u}_d(t+k-h_i) \right) \quad (7)$$

with $h_p = \max_{i \in [1, p]} (h_p(i))$. The minimization of (7) will be done under the following hypothesis

$$\bar{u}_d(t+k) = 0 \quad \forall k \in [h_c \dots h_p] \quad (8)$$

where h_c is the control horizon.

3.3 J-step ahead optimal output prediction

Using (4), the exact value of the outputs at time $(t+k)$, i.e. $\bar{y}(t+k)$ is given by

$$\begin{aligned} \bar{y}(t+k) &= HF^k X(t) + \sum_{i=1}^k HF^{k-i} G \bar{u}_d(t+i-1) \\ &+ HF^{k-1} E \bar{\gamma}(t) + \sum_{i=2}^k HF^{k-i} E \bar{\gamma}(t+i-1) \\ &+ \bar{\gamma}(t+k) \end{aligned} \quad (9)$$

The optimal prediction of $\bar{y}(t+k)$ can then be computed as follows

$$\begin{aligned} \hat{\bar{y}}(t+k/t) &= HF^k \hat{X}(t/t) + \sum_{i=1}^k HF^{k-i} G \bar{u}_d(t+i-1) \\ &+ HF^{k-1} E \hat{\bar{\gamma}}(t/t) \end{aligned} \quad (10)$$

where $\hat{X}(t/t)$ denotes an estimation of $X(t)$ using all the available signals at time t that can be delivered by a Kalman filter and, using (4), $\hat{\bar{\gamma}}(t/t) = \bar{y}(t) - H \hat{X}(t/t)$. One finally gets

$$\begin{aligned} \hat{\bar{y}}(t+k/t) &= HF^{k-1} (F - EH) \hat{X}(t/t) \\ &+ \sum_{i=1}^k HF^{k-i} G \bar{u}_d(t+i-1) + HF^{k-1} E \bar{y}(t) \end{aligned} \quad (11)$$

Let us now define $\hat{Y}(t+h_p/t)$, $\hat{Y}_j(t+h_p(j)/t)$ and $U_d(t+h_c-1)$ by

$$\begin{cases} \hat{Y}(t+h_p/t) &= [\hat{\bar{y}}^T(t+h_i/t) \dots \hat{\bar{y}}^T(t+h_p/t)]^T \\ \hat{Y}_j^T(t+h_p(j)/t) &= [\hat{y}_j^T(t+h_i/t) \dots \hat{y}_j^T(t+h_p(j)/t)]^T \\ U_d(t+h_c-1) &= [\bar{u}_d^T(t) \dots \bar{u}_d^T(t+h_c-1)]^T \end{cases} \quad (12)$$

where $\hat{y}_j(t+k/t)$ is the prediction of the j^{th} output at time $(t+k)$. The predictions of the vector of outputs from $(t+h_i)$ to $(t+h_p)$ can then be written under the following matrix form

$$\begin{aligned} \hat{Y}(t+h_p/t) &= GU_d(t+h_c-1) + \Phi(F-EH) \hat{X}(t/t) \\ &+ \Phi E \bar{y}(t) \end{aligned} \quad (13)$$

with

$$\begin{cases} G = \begin{pmatrix} HF^{h_i-1}G & \dots & HG & 0 & \dots & 0 \\ HF^{h_i}G & \dots & \dots & HG & \dots & 0 \\ \dots & \dots & \dots & \dots & \dots & \dots \\ HF^{h_p-1}G & \dots & \dots & \dots & \dots & HF^{h_p-h_c}G \end{pmatrix} \\ \Phi = \begin{pmatrix} HF^{h_i-1} \\ HF^{h_i} \\ \vdots \\ HF^{h_p-1} \end{pmatrix} \end{cases} \quad (14)$$

and the set of predictors of the j^{th} output is given by

$$\begin{aligned} \hat{Y}_j(t+h_p(j)/t) &= G_j U_d(t+h_p-1) \\ &+ \Phi_j (F-EH) \hat{X}(t/t) + \Phi_j E \bar{y}(t) \end{aligned} \quad (15)$$

with

$$\begin{aligned} G_j &= \begin{pmatrix} G(j,:) \\ G(p+j,:) \\ \vdots \\ G(p \times h_p(j) + j,:) \end{pmatrix} \\ \Phi_j &= \begin{pmatrix} \Phi(j,:) \\ \Phi(p+j,:) \\ \vdots \\ \Phi(p \times h_p(j) + j,:) \end{pmatrix} \end{aligned} \quad (16)$$

where $G(j, :)$ and $\Phi(j, :)$ are the j^{th} line of the matrices G and Φ respectively.

Remark 3.1. Using (9) and (10), the prediction error $\tilde{y}(t+k/t) = \bar{y}(t+k) - \hat{y}(t+k/t)$ can be expressed as follows

$$\begin{aligned}\tilde{y}(t+k/t) &= HF^k \left(X(t) - \hat{X}(t/t) \right) \\ &+ HF^{k-1} E (\bar{\gamma}(t) - \hat{\gamma}(t)) \\ &+ \sum_{i=2}^k HF^{k-i} E \bar{\gamma}(t+i-1) + \bar{\gamma}(t+k)\end{aligned}\quad (17)$$

This clearly shows that the prediction error does not depend on the future control values and hence the vector $U_d(t+h_c-1)$ that minimizes J_2 also minimizes the following criteria

$$\begin{aligned}\hat{J}_2 &= \sum_{j=1}^p \sum_{k=h_i}^{h_p(j)} \hat{y}_j^T(t+k/t) q_j \hat{y}_j(t+k/t) \\ &+ \sum_{k=h_i}^{h_p} \bar{u}_d^T(t+k-h_i) R \bar{u}_d(t+k-h_i)\end{aligned}\quad (18)$$

3.4 Multivariable output feedback control law design

Using the notations (12), the criteria (18) can be written as follows

$$\begin{aligned}\hat{J}_2 &= \sum_{j=1}^p \hat{Y}_j^T(t+h_p(j)/t) q_j \hat{Y}_j(t+h_p(j)/t) \\ &+ U_d^T(t+h_c-1) Z U_d(t+h_c-1)\end{aligned}\quad (19)$$

with $Z = I_{h_c} \otimes R$ where \otimes denotes the Kronecker product. Introducing (15) in (19) leads to

$$\begin{aligned}\hat{J}_2 &= \sum_{j=1}^p (G_j U_d(t+h_c-1) + F_j)^T q_j \\ &\quad (G_j U_d(t+h_c-1) + F_j) \\ &\quad + U_d^T(t+h_c-1) Z U_d(t+h_c-1)\end{aligned}\quad (20)$$

with

$$F_j = \Phi_j (F - EH) \hat{X}(t/t) + \Phi_j E \bar{y}(t) \quad (21)$$

The control vector $U_d(t+h_c-1)$ that minimizes \hat{J}_2 is such that $\frac{\partial \hat{J}_2}{\partial U_d(t+h_c-1)} = 0$ which gives

$$\left(Z + \sum_{j=1}^p q_j G_j^T G_j \right) U_d(t+h_c-1) = - \sum_{j=1}^p q_j G_j^T F_j \quad (22)$$

hence,

$$U_d(t+h_c-1) = - \left(Z + \sum_{j=1}^p q_j G_j^T G_j \right)^{-1} \left(\sum_{j=1}^p q_j G_j^T F_j \right) \quad (23)$$

The multivariable linear time invariant receding horizon control law is then given by

$$\begin{aligned}\bar{u}_d(t) &= -\Gamma (F - EH) \hat{X}(t/t) - \Gamma E \bar{y}(t) \\ &= -K_1 \hat{X}(t/t) - K_2 \bar{y}(t)\end{aligned}\quad (24)$$

where $\Gamma \in$ is composed of the m first lines of the matrix $\left(Z + \sum_{j=1}^p q_j G_j^T G_j \right)^{-1} \left(\sum_{j=1}^p q_j G_j^T \Phi_j \right)$ and

$$\begin{cases} K_1 = \Gamma (F - EH) \\ K_2 = \Gamma E \end{cases} \quad (25)$$

3.5 Linear time-invariant controller

The stationary Kalman filter associated to the innovation state-space model (4) is given by ([3])

$$\begin{cases} \hat{X}(t/t) &= \hat{X}(t/t-1) \stackrel{def}{=} \hat{X}(t) \\ \hat{X}(t+1) &= F \hat{X}(t) + G \bar{u}_d(t) + E (\bar{y}(t) - H \hat{X}(t)) \\ &= (F - EH) \hat{X}(t) + G \bar{u}_d(t) + E \bar{y}(t) \end{cases} \quad (26)$$

On the other hand, the state-space model that relates $\bar{u}_d(t)$ and $\bar{u}(t)$ in the particular case of a step-like disturbance multivariable model is the following one

$$\begin{cases} X_d(t+1) &= X_d(t) + \bar{u}_d(t) \\ \bar{u}(t) &= X_d(t) + \bar{u}_d(t) \end{cases} \quad (27)$$

where $X_d(t)$ denotes the state vector of the disturbance model. Introducing the control law (24) in (27) and using (26) leads to the state-space structure of the controller i.e

$$\begin{cases} \begin{pmatrix} \hat{X}(t+1) \\ X_d(t+1) \end{pmatrix} = \begin{pmatrix} F - EH - GK_1 & 0 \\ 0 & I_m \end{pmatrix} \begin{pmatrix} \hat{X}(t) \\ X_d(t) \end{pmatrix} \\ \quad + \begin{pmatrix} E - GK_2 \\ 0 \end{pmatrix} \bar{y}(t) \\ \bar{u}(t) = \begin{pmatrix} -K_1 & I \end{pmatrix} \begin{pmatrix} \hat{X}(t) \\ X_d(t) \end{pmatrix} + \begin{pmatrix} -K_2 \\ 0 \end{pmatrix} \bar{y}(t) \end{cases} \quad (28)$$

4 Experimental results

The identified model in cascade with the state-space model of a multivariable integrator led to the matrices F , G and H of the extended model (4) for the draw tower process. The parameters of the control law have been specified such as to ensure a satisfying shaping

of the sensitivity functions. Please note that the prediction horizons are quite different for the 2 outputs as it was expected. The observer dynamic has been adjusted according to a robust pole placement method whose design parameter is the observation horizon T_o ([5]). This led to the following design parameters values.

$$\begin{cases} T_o = 8, h_p(1) = 10, h_p(2) = 25, h_i = 1, h_c = 2 \\ R = \begin{pmatrix} 12.9 & 0 \\ 0 & 74.1 \end{pmatrix}, Q = \begin{pmatrix} 25.25 & 0 \\ 0 & 25 \end{pmatrix} \end{cases} \quad (29)$$

The corresponding output and input sensitivity functions, respectively $(I_2 + \text{Process} \times \text{Controller})^{-1}$ and $(I_2 + \text{Controller} \times \text{Process})^{-1}$ and reported on figures (6) and (7) and show that the usual robustness criteria are fulfilled. Moreover, the sensitivity function $\text{Input Sensitivity} \times \text{Controller}$, reported on figure (5), indicates that the control variables should not be too much sensitive to noisy measurements. Finally, a two-degree of freedom controller has been synthesized using a *Partial State Reference Model Control* approach to deal with a drawing speed tracking objective ([12]). The input/output performances have been reported on figures (2), (3), (4) and (5). For confidentiality purposes, the magnitude of the different signals have been normalized and expressed in percent of the nominal point. The results clearly show the capacity of the control scheme to efficiently reject disturbances and the tracking objective is also correctly achieved. The drawing speed is controlled with a precision within $\pm 2\%$ of the nominal value. Please note finally that the control variables are quite insensitive to the high level of measurement noise despite the poor quality of the fiber tension signal.

5 Conclusion

In this paper, a multivariable control law for a draw tower process has been proposed. The difference in the range of the dynamics of the plant outputs (drawing speed and fiber tension) and in the measurements noise variances motivated the design of a control law that enables to specify independently the closed loop dynamics of those variables. For that purpose, a multivariable predictive control law with separate prediction horizons has been designed using a state-space approach. The design parameters have been chosen in such a way that a correct shaping of the sensitivity functions is achieved. The performances of the algorithm have been experimentally evaluated.

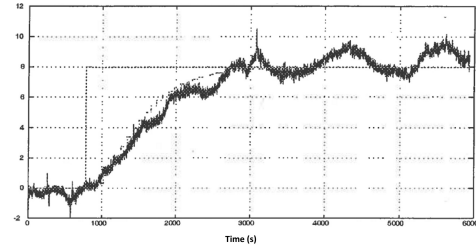


Figure 2: Drawing speed $y_1(t)$ and its tracking reference (—)

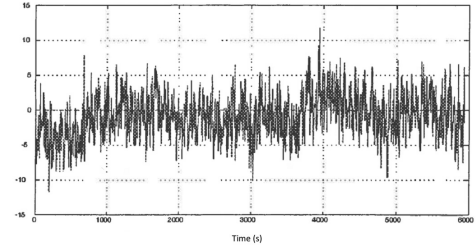


Figure 3: Fiber tension $y_2(t)$

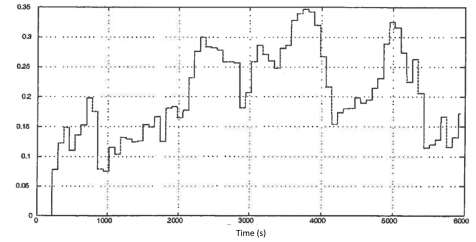


Figure 4: Preform downfeed speed $u_1(t)$

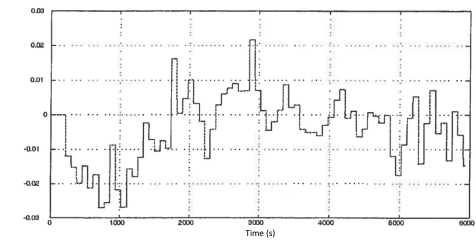


Figure 5: Furnace heat power $u_2(t)$

References

- [1] B.D.O. Anderson and J.B. Moore. *Optimal Filtering*. Prentice Hall, 1979.
- [2] G. W. Barton, S. H. Law, P. McNamara, and T. N. Phan. Measurement and control challenges for the

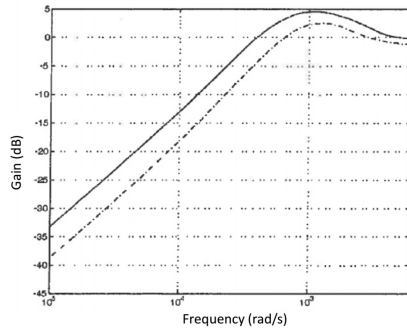


Figure 6: Sensitivity function

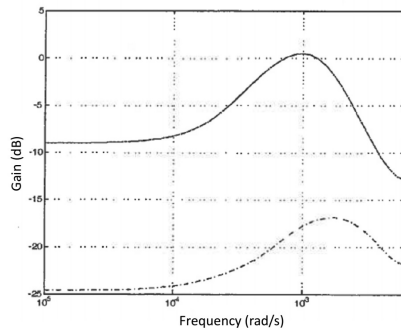


Figure 7: Input sensitivity function

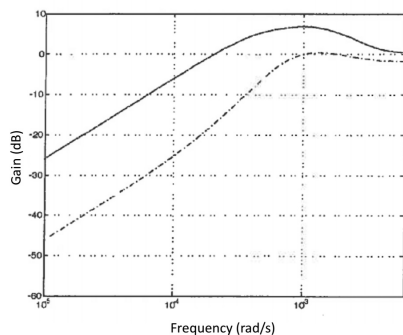


Figure 8: Sensitivity function \times Controller

specialty optical fibre industry in the 21st century. In *5th IEEE Asian Control Conference*, volume 2, pages 1137–1144, 2004.

- [3] P.E. Caines. Relationship between Box-Jenkins-Åström control and Kalman linear regulator. *Proceedings of the Institution of Electrical Engineers*, 119(5):615–620, 1972.
- [4] E.C. Camacho and C. Bourdons. *Model Predictive Control*. Springer Verlag, 1999.
- [5] J. Chebassier. *Méthodologies pour la conception d'un système de commande par ordinateur*. PhD thesis, Institut National Polytechnique de Grenoble, 1999.
- [6] Shuai Ci-jun, Duan Ji-an, and Zhong Jue. Effect of technological parameters on optical performance of fiber coupler. *Journal of Central South University of Technology*, 14:370 – 373, 2007.
- [7] HD.W. Clarke and C. Mothadi. Generalized predictive control. *Automatica*, 23:137–160, 1987.
- [8] J.-P. Corriou. *Process Control-Theory and Applications*. Springer Verlag, 2004.
- [9] P. Dorleans, O. Gehan, E. Pigeon, M. M'Saad, M. Hertz, and M. Desalle. Diameter regulation of an optical fiber using a generalized predictive control approach. In *Proc. of the 14th IFAC world congress*, 1999.
- [10] L. Grüne and J. Pannek. *Nonlinear Model Predictive Control*. Springer Verlag, 2011.
- [11] J.M. Maciejowski. *predictive control with constraints*. Prentice Hall, 2002.
- [12] M. M'Saad and G. Sanchez. Partial state model reference adaptive control of multivariable systems. *Automatica*, 28:1189–1197, 1992.
- [13] P. Van Overschee and B. De Moor. N4sid : subspace algorithms for the identification of combined deterministic-stochastic systems. *Automatica*, 30:75–93, 1994.
- [14] J.B. Rawlings and D.Q. Mayne. *Model predictive control : theory and design*. North Hill publication, 2009.
- [15] Paul S. Oh, John J. Mcalarnay, and Dilip K. Nath. Effect of fiber drawing tension on optical and mechanical properties of optical fiber waveguides. *Journal of the American Ceramic Society*, 66:C84 – C85, 2006.